

DYNAMIC BEHAVIOR OF SHEET PILE QUAY WALL STABILIZED BY SEA-SIDE GROUND IMPROVEMENT

M. Ruhul Amin KHAN¹, Kimitoshi HAYANO², Masaki KITAZUME³

ABSTRACT

Sea-side ground improvement is one of the techniques to increase seismic stability which will not interrupt the port-side activities during its execution. A centrifuge model shaking test was conducted at the Port and Airport Research Institute, Yokosuka, Japan to investigate the dynamic response of sheet pile quay wall set on a thick clay deposit. An area at the sea-side adjacent to the quay wall was improved with cement-treated Kawasaki clay. Under 50g centrifugal acceleration, the clay deposit was consolidated and four stages of shaking were applied to the quay wall. Sinusoidal input accelerations at 2 Hz were 45, 196, 294 and 343 Gal (in prototype scale). The recorded input-output accelerations, deflection of the quay wall, earth pressures along depth and pore pressures were used to evaluate the behavior of the sheet pile quay wall stabilized by the sea-side ground improvement. The results of the study indicated that an improved area provides significant resistance against seismic load; deflection of the quay wall is restricted to 0.68 m at 343 Gal acceleration and the maximum flexural stresses are developed at the middle of embedded part of the sheet pile wall.

Keywords: Centrifuge model test, sheet pile quay wall, ground improvement, seismic loading, CDM

INTRODUCTION

Different degrees of rotation, horizontal displacement and structural failure during earthquakes are the major causes of damage to sheet pile quay walls. The seismic stability of a sheet pile quay wall can generally be improved by: (i) increasing the effective angle of internal friction or cohesion of the backfill soil, (ii) driving the sheet pile into a dense layer of sand, (iii) replacing sheet piles, (iv) supporting the wall by additional ties or anchorages. Watabe et al., 2006 showed the effective seismic performance of an anchored sheet pile quay wall backfilled with light weight materials. They performed a series of centrifuge shaking table tests. There is ample evidence from devastating 1995 Nanbu (Kobe), Hyogo ken, Japan, 1999 Kocaeli, Turkey and 1999 Chi-Chi, Taiwan earthquakes that improved sites suffer less ground deformation and subsidence than adjacent unimproved areas. The studies of the events clearly indicate that ground improvement reduces large ground displacements during seismic motion. Kitazume et al., 2002 performed a series of centrifuge model test on failure pattern and earth pressure of cement treated ground behind a caisson-type quay wall under seismic loading. The improved backfill ground reduced the earth pressure on the quay wall and the horizontal deflection of the quay wall as well.

Most of the mentioned techniques require large efforts and time, especially in the case of an existing quay wall. For an existing quay wall, it would be preferable not to close the port for a long period.

¹ Researcher, Soil Stabilization Division, Port and Airport Research Institute, 3-1-1 Nagase, Yokosuka 239-0826, Japan, Email: khan@pari.go.jp

² Senior Researcher, Soil Stabilization Division, Port and Airport Research Institute, 3-1-1 Nagase, Yokosuka 239-0826, Japan, Email: hayano@pari.go.jp

³ Head, Soil Stabilization Division, Port and Airport Research Institute, 3-1-1 Nagase, Yokosuka 239-0826, Japan, Email: kitazume@pari.go.jp

Sea-side ground improvement is one of the techniques which will not interrupt the port-side activities during its execution. The sea-side ground improved with cement deep mixing (CDM) (CDIT, 2002) was studied by Khan et al., 2006 through a series of centrifuge model tests. The stability of the sea-side improved pseudo-statically loaded sheet pile quay wall was investigated in the study.

A centrifuge model shaking table test which is different from pseudo-static test was conducted to investigate the dynamic response of sheet pile quay wall. The sheet pile quay wall studied here is without anchorage and tie and embedded in a thick clay deposit. An area at the sea-side adjacent to the quay wall was improved with cement-treated Kawasaki clay. Under 50g centrifugal acceleration, the clay deposit was consolidated and four stages of shaking were applied to the quay wall. Applied sinusoidal input accelerations were 45, 196, 294 and 343 Gal at frequency of 2 Hz. The aim of the centrifuge shaking table test is to explore the dynamic behavior of sheet pile quay wall improved with sea-side cement deep mixing (CDM).

The time period of shaking is scaled by $1/N$ to produce waves with N times greater acceleration, N times smaller displacement and equal stress to those in the prototype. Scaling conflicts between the time rate of cyclic loading and the dissipation of pore water pressure can be resolved by reducing the permeability by N by using a pore fluid with viscosity N times that of water (Stewart et al., 1998). The test was performed on the 306g-ton centrifuge at the Port and Airport Research Institute, Yokosuka, Japan. The centrifuge has an effective radius of 3.8 m, maximum acceleration of 113 g and maximum payload of 2.7 ton.

CENTRIFUGE MODEL DESCRIPTION

Model set-up

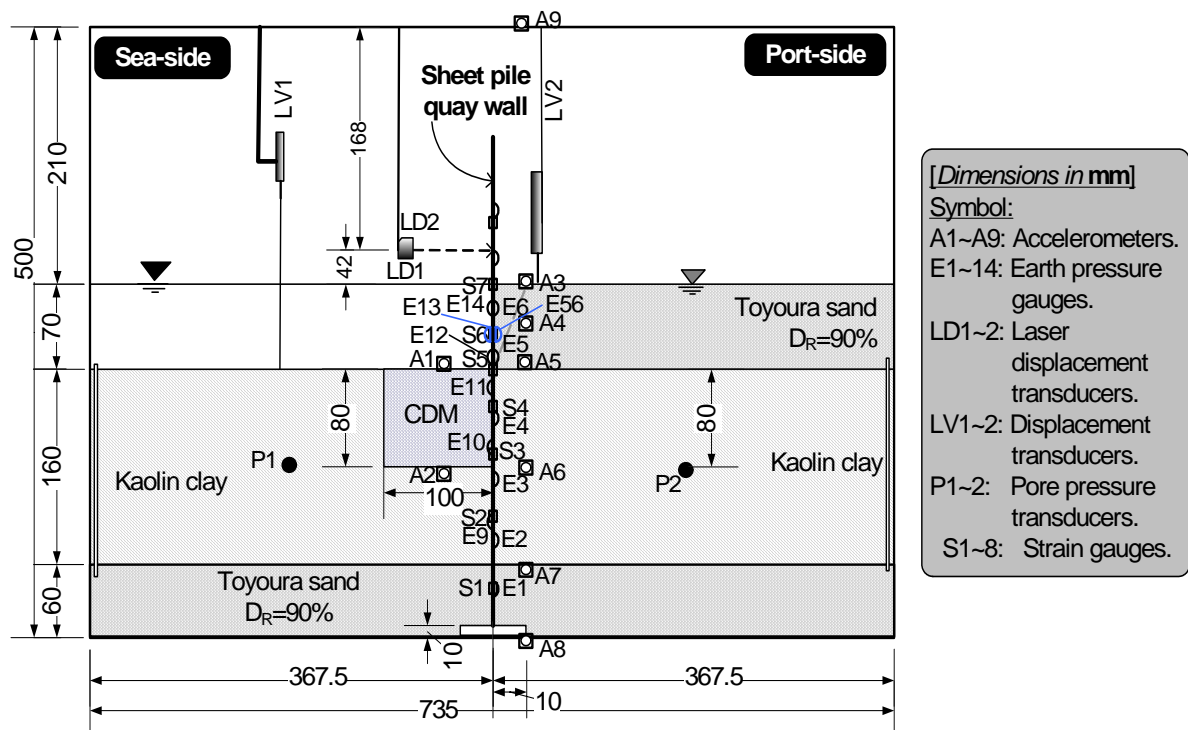


Figure 1. Schematic illustration of model set-up

Figure 1 shows the schematic illustration of the model set-up. A strong box of 735 mm length, 500 mm depth and 200 mm breadth with a transparent front window was used for the test. Wave absorbing

materials were set on 200 mm faces of the strong box. Photos of model set-up are shown in Fig. 2. The model sheet pile quay wall is a 3 mm thick steel plate instrumented with 8 pair of strain gauges (S1 to S8) and 15 earth pressure gauges (E1 to E14 & E56) on both sides. At the bottom of the strong box, the sheet pile wall is set on a 10 mm thick rough surfaced acrylic plate and at the top it is clamped with guide plates, so that it is firmly fixed and remains vertical.

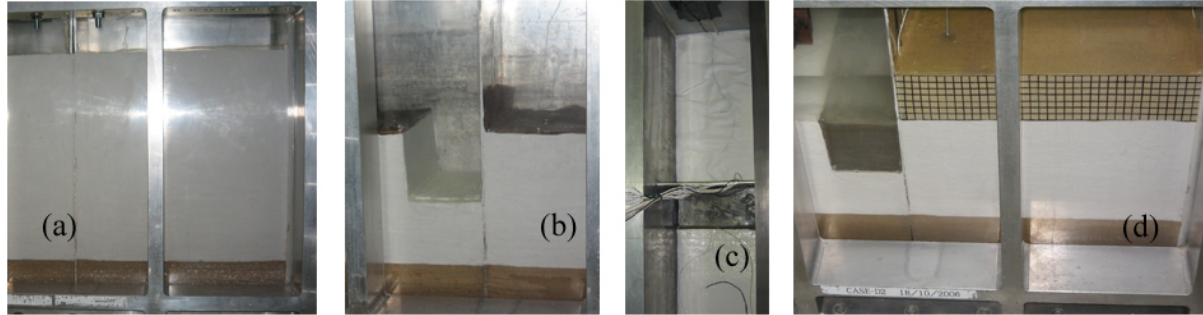


Figure 2. Construction stages photographs: (a) kaolin clay slurry is poured until the top of the strong box, (b) CDM hole is excavated in the consolidated clay, (c) top view of the model showing the CDM, sheet pile wall and white kaolin, and (d) final model with backfill sand and sea-side water

Table 1. Properties of kaolin clay and Toyoura sand

Kaolin clay		Toyourea sand	
Liquid limit, W_L (%)	59.3	Specific gravity, G_s	2.65
Plastic index, I_p (%)	33.0	D_{50} (mm)	0.19
Specific gravity, G_s	2.72	Coefficient of Uniformity, C_u	1.56
Compression index, C_c	0.49	Friction angle ϕ'	42°

The model sand ground of 60 mm thick and 90% relative density was prepared by pouring dry Toyoura sand using a sand hopper. Properties of the kaolin clay and Toyoura sand are shown in Table 1. The remolded clay slurry (water content of 120%) was then poured over the saturated sand layer in the strong box (Fig. 2(a)). Pre-consolidation was carried out by compressing the clay with two bellofram cylinders. The successive consolidation pressures applied were 1 kPa, 5 kPa, 10 kPa, 20 kPa, 40 kPa, 80 kPa and 150 kPa. Primary consolidation was achieved in each stage. After having completed the consolidation on the laboratory floor the surface of consolidated clay was skimmed off to a depth of 160 mm. A specified area, 100 mm \times 80 mm (Fig. 2(b), (c)) in sea-side adjacent to the sheet pile was excavated. Cement treated Kawasaki clay was poured into the excavation. Kawasaki clay slurry with 130% water content was thoroughly mixed with Portland cement that is 40% of dry weight of Kawasaki clay. Sufficient water was added on top of the clay and CDM for curing. Seven days curing was allowed to gain strength (unconfined compression strength, $q_u \approx 1340$ kPa) by the CDM. In the port-side, 0.2 mm thick and 70 mm height rubber membranes were pasted on the greased surfaces (front and back sides) of the strong box. A 10 mm square mesh was drawn on the front membrane (Fig. 2(d)). The backfill sand of 70 mm thick and 90% relative density was prepared by pouring dry Toyoura sand in the port-side using a sand hopper. Care was taken in saturating the backfill with water at modest hydraulic gradient. Water was supplied in the sea-side until the height becomes 70 mm (Fig. 2(d)). As shown in Fig. 1, two displacement transducer (LV1-2), two laser displacement transducers (LD1-2), two pore pressure transducers (P1-2) and nine accelerometers (A1-9) were firmly and properly set on the strong box and into the ground.

Test procedures and conditions

The strong box with the model was mounted on the swinging platform of the centrifuge. Centrifugal acceleration was increased up to 50 g. At 50 g, the bottom sand layer becomes 3 m, clay depth becomes 8 m, backfill and sea water heights become 3.5 m and CDM area becomes 5 m \times 4 m. The

consolidation in the centrifuge at 50 g was conducted until the degree of consolidation was estimated to have achieved 90%. Data from the pore pressure transducers in the clay and LV1-2 were used to estimate the degree of consolidation. At 50 g, four shaking events were applied to this model in flight. The shaking was applied parallel to the long side of the strong box. Four shaking stages were applied at 2 Hz (100 Hz in model) and in 50 sinusoidal cycles. Magnitudes of shaking were 45 Gal, 196 Gal, 294 Gal and 343 Gal (2.3g, 10g, 15g and 17.5g in model).

Deflection of sheet pile quay wall, pore water pressures in the ground, earth pressures at various elevations and strains on the surface of the sheet pile wall were monitored during the test. The positions of the sensors are shown in Fig. 1. Still pictures of the model were taken before and after the each shaking. All the test results in the following sections are presented in the prototype scale.

TEST RESULTS AND DISCUSSIONS

Stress history and strength profile

The seashore may consist of a thick clay layer underlain by a sand layer. Highly overconsolidated (OC) clay is chosen to facilitate the model preparation. The maximum effective past pressure experienced by the clay can be assumed to be the same as that applied to consolidate the clay, i.e. 150 kPa. The sheet pile is set-up to a certain depth into the strata of sand underlying the clay to ensure firm fixity of the quay wall. Stress history of the clay layer is shown in Fig. 3. In the figure, σ_v' and σ_p' are the current effective vertical stress and the past maximum vertical consolidation pressure respectively; OCR is the overconsolidation ratio (σ_p'/σ_v'); the coefficient of in-situ earth pressure, K_0 , is derived for overconsolidated (OC) clay with a critical state friction angle $\phi'=28.6^\circ$, following the equation presented by Mayne and Kulhawy (1982):

$$K_{0(OC)} = (1 - \sin \phi') OCR^{\sin \phi'} \quad (1)$$

The undrained shear strength, c_u , of the clay is derived from the formula of Wroth (1984):

$$\frac{c_u}{\sigma_v'} = \left(\frac{c_u}{\sigma_v'} \right)_{NC} OCR^m \quad (2)$$

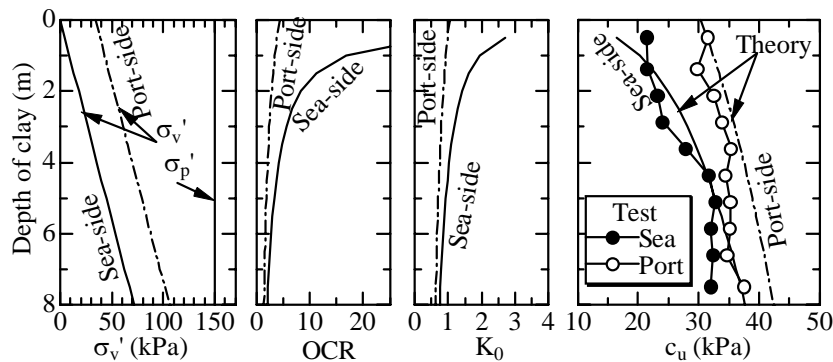


Figure 3. Stress history and undrained shear strength of the clay stratum

where NC = normally consolidated clay, with an experimental value of $(c_u/\sigma_v')_{NC} = 0.314$ and $m = 0.75$. Theoretical c_u values have been compared with the test results. After completion of the centrifuge test the water content profile of the clay ground were measured. The c_u profile along the depth is estimated from the water content profile both in the sea-side and port-side and shown in Fig. 3. Although the clay samples were collected after the loading stage, the values estimated from the test

results compares fairly well with the theoretical c_u values (Fig. 3), which were predicted before the loading stage.

Deflection of sheet pile quay wall

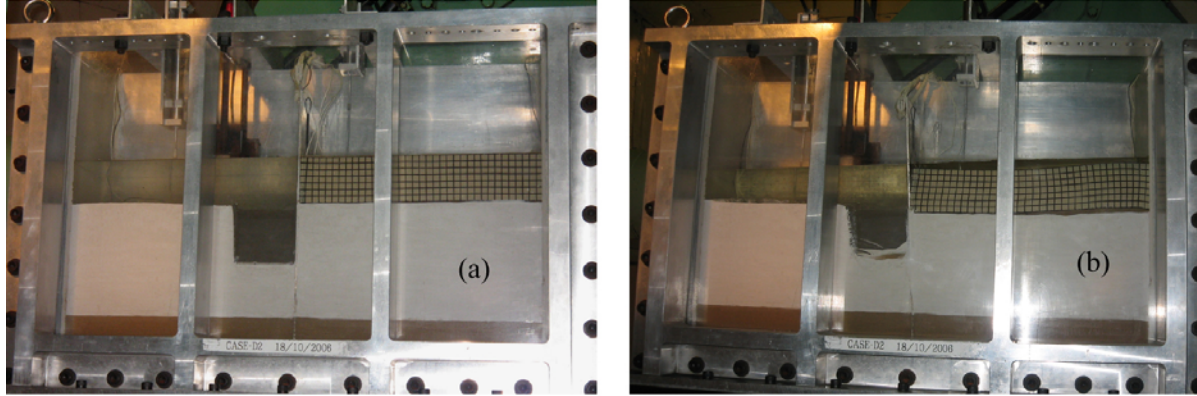


Figure 4. Photos of the model: (a) the initial condition and (b) 343 Gal shaking stage

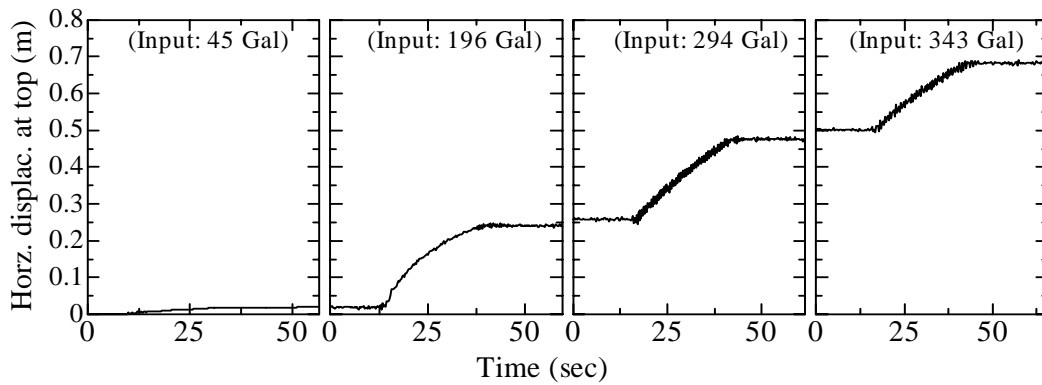


Figure 5. Horizontal deflection of quay wall at backfill surface level in different shaking stages

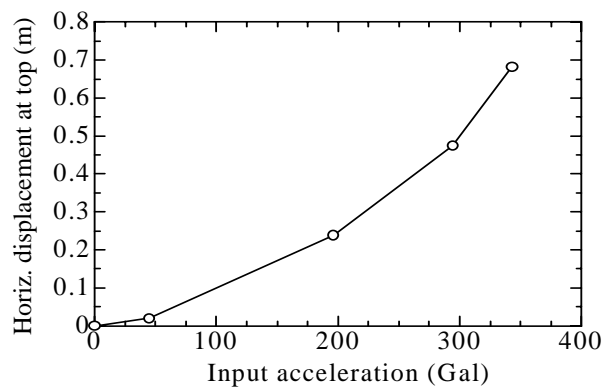


Figure 6. Horizontal deflection of quay wall at backfill surface level versus input acceleration

Deflection of the sheet pile quay wall is the main index in describing stability. Figures 4(a) and (b) show the photos of the model at the initial condition and 343 Gal shaking stage respectively. Deflection of the sheet pile wall from the vertical position, shearing and subsidence of the backfill sand can be seen in the photos. Figure 5 shows the horizontal deflection of the quay wall at backfill surface level, δ , in different input shakings. Successive deflections at 45 Gal, 196 Gal, 294 Gal, and 343 Gal shaking were measured as 0.02m, 0.24m, 0.47m and 0.68m respectively. It is found by Khan

et al., 2006 that stiffness of the sea-side improved quay wall becomes almost four times larger than that of the unimproved sea-side ground under the static loading condition. Here stiffness is indicated as horizontal load per unit deflection. In the first two shakings the quay wall showed larger stiffness. However, the interaction between the quay wall and the CDM, and between the CDM and the surrounding clay are not yet thoroughly investigated. These interaction processes can affect the deflection of the quay wall significantly. The relationship between the horizontal deflection of the quay wall, δ , and input acceleration is shown in Fig. 6. Deflection increases with the increases of acceleration and shows a nonlinear relationship.

Excess pore water pressure

Although a pore fluid with viscosity of 50 times that of water would be necessary to satisfy the scaling laws (at 50g) as discussed in the previous section, tap water was used to saturate the backfill and to fill the sea-side, thus increasing the rate of dissipation of excess pore water pressure by a factor of 50. Excess pore water pressure ratio is computed by dividing the generated excess pore water pressure by the initial effective overburden stress.

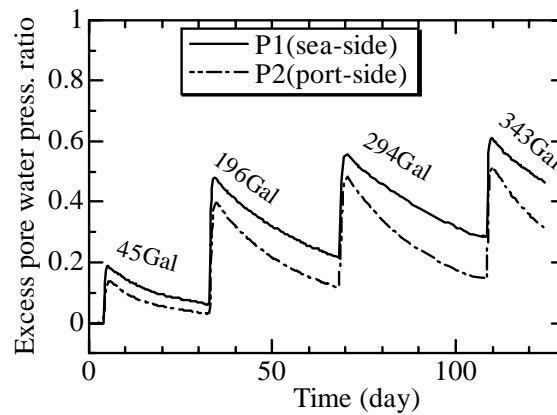


Figure 7. Excess pore water pressure during the shakings

Figure 7 shows the excess pore water pressure development in the sea-side and port-side during all of the four shakings. Pore pressure transducers, P1 and P2 were set at the mid of clay in both the sea-side and port-side. The excess pore water pressure ratio quickly rises to the peak at the start of shaking and gradually dissipates with time. Maximum pore pressure ratio observed is about 0.6. It can be seen from the plot that after each shaking some amount of residual excess pore water pressure remains in the ground. This residual pressure may affect the stiffness of the ground during other seismic motions. During large acceleration it can weaken the shear stress transmission inside the ground though one step shaking at larger acceleration might have different behavior.

Acceleration time histories

As shown in Fig. 1, accelerations were recorded at various points throughout the model. Figures 8 and 9 illustrate the difference in response recorded in 45 Gal, 196 Gal and 343 Gal shaking stages. At 45 Gal shaking it is apparent that the motion is significantly thickened from the bottom of the clay layer to the top of backfill sand. Accelerometers A1 and A2 (CDM zone) were placed almost in the same level as A5 and A6 (port-side clay). It can be seen from Figs. 8(a) and 9(a) that the acceleration histories in A1, A2 and A5, A6 are almost similar in the first stage of shaking. Initially the clay, CDM and sand layers were well integrated. The initial stiffness of the sheet pile quay wall system was larger and different in the subsequent loading stages, so that the motion in 343 Gal stage is different and weakened from the bottom of the clay to the top of the backfill sand. In 196 Gal shaking stage (Fig. 8(b) and 9(b)), the base, clay bottom and backfill top felt relatively strong motion.

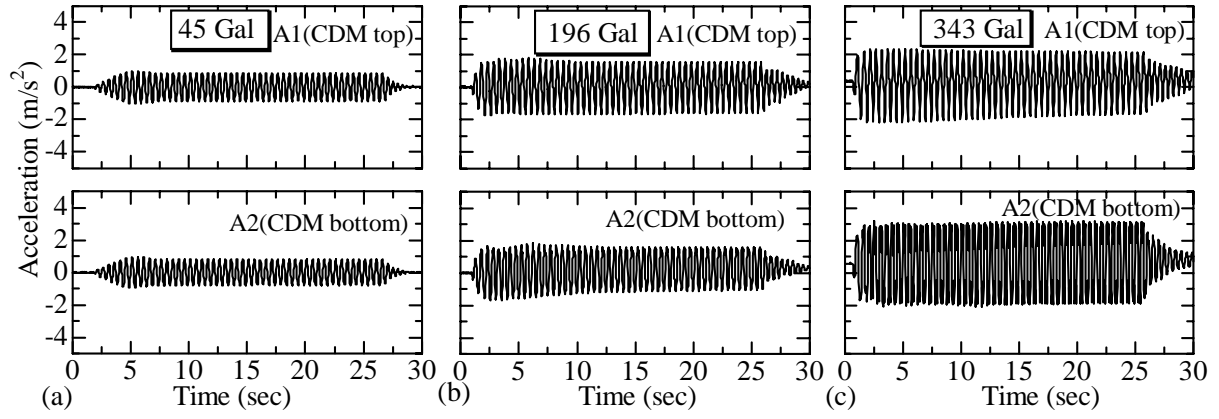


Figure 8. Acceleration time histories at top and bottom of the CDM for: (a) 45 Gal, (b) 196 Gal and (c) 343 Gal shaking

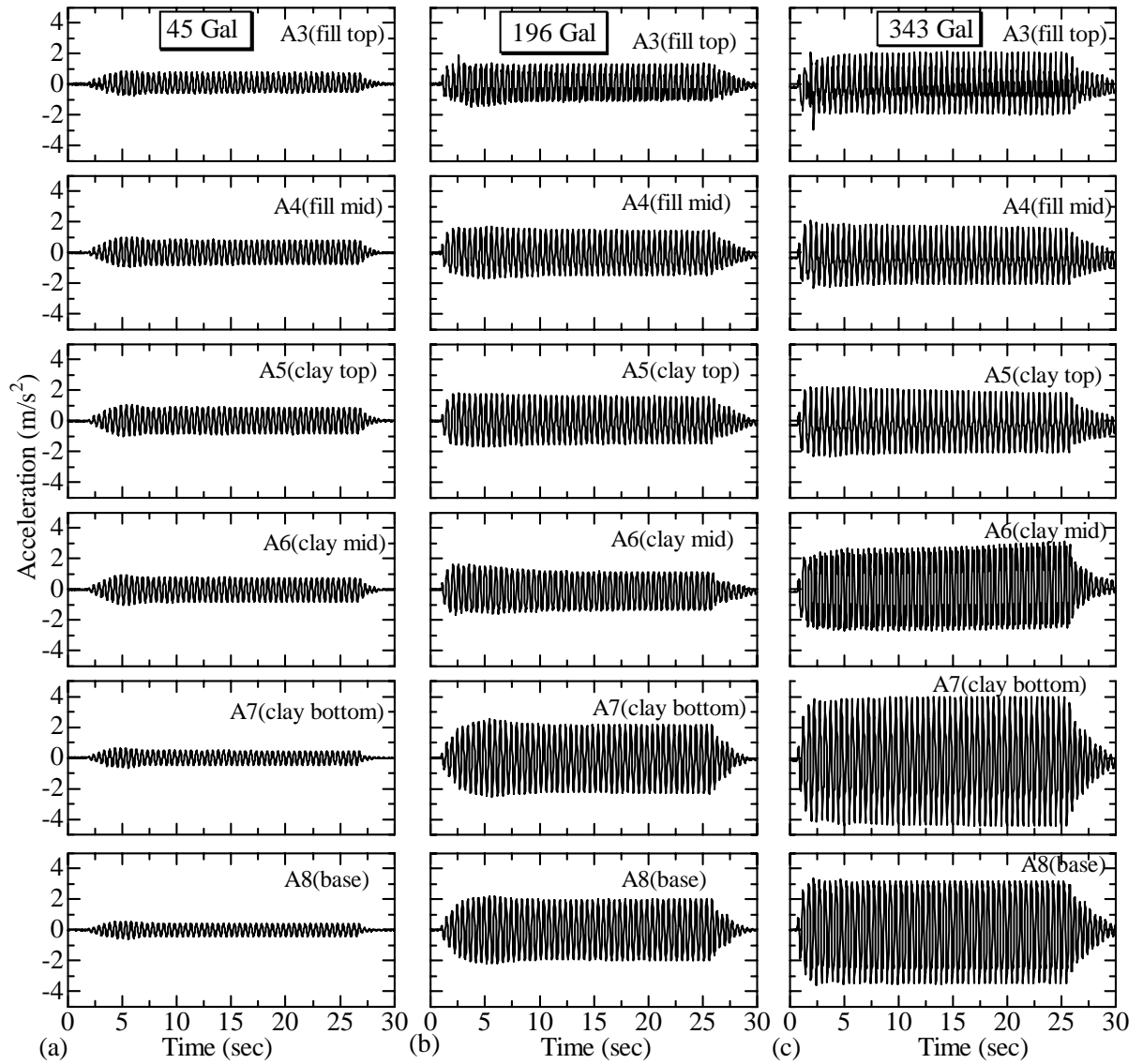


Figure 9. Acceleration time histories in the port-side ground for: (a) 45 Gal, (b) 196 Gal and (c) 343 Gal shaking

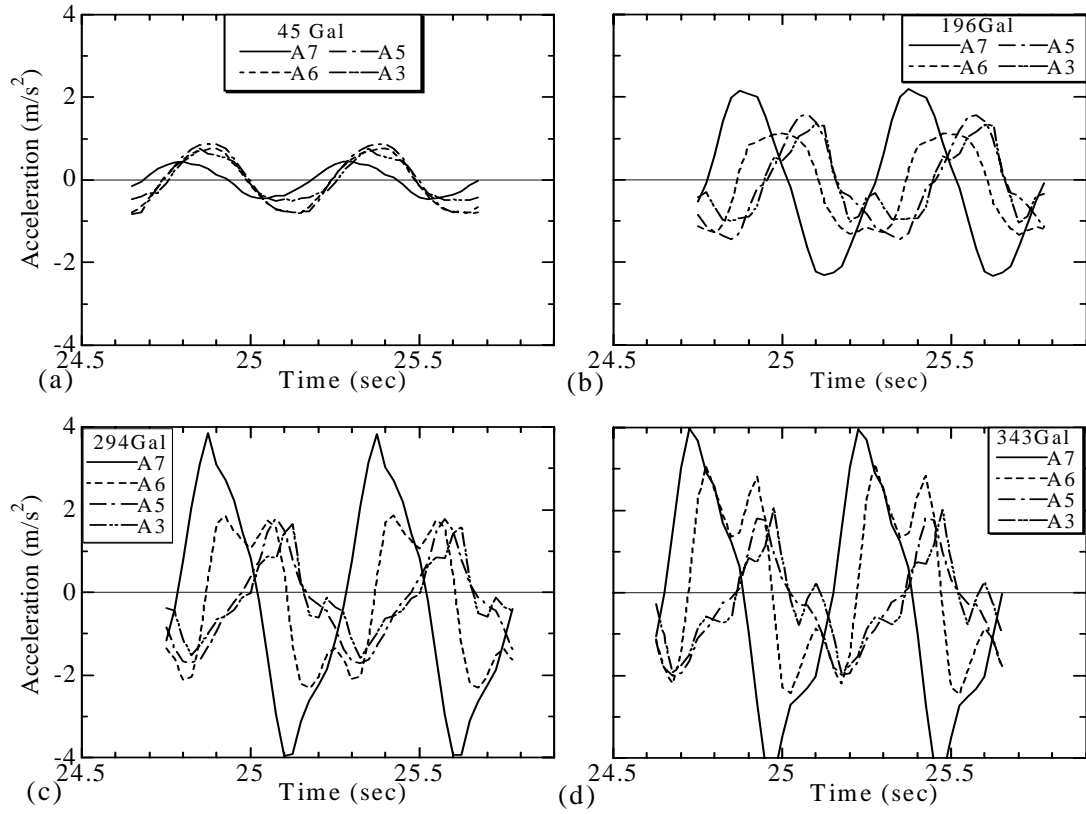


Figure 10. Acceleration time lag in the port-side at final phases of: (a) 45 Gal, (b) 196 Gal, (c) 294 Gal and (d) 343 Gal shaking

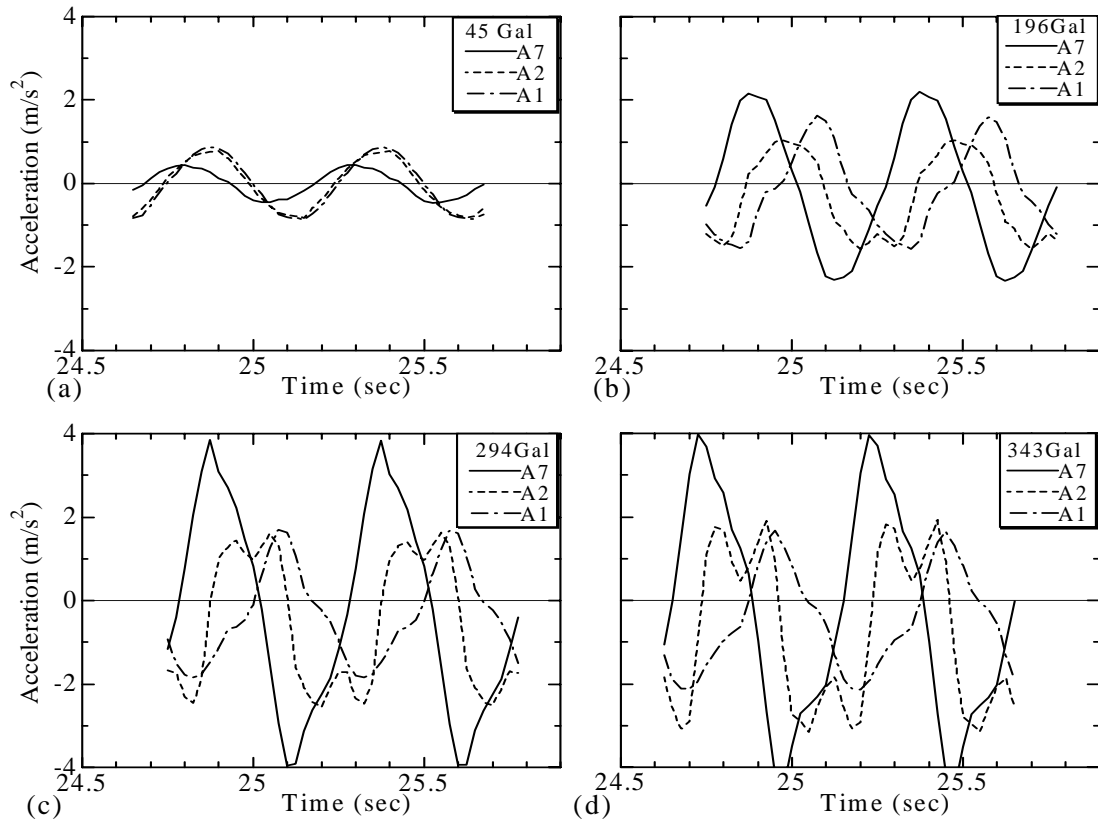


Figure 11. Acceleration time lag in the sea-side at final phases of: (a) 45 Gal, (b) 196 Gal, (c) 294 Gal and (d) 343 Gal shaking

Figures 10 and 11 show the time lag in acceleration-waves that are generated in the port-side and sea-side respectively. Acceleration in the port-side is considered at the bottom sand (A7), the clay-mid (A6), the clay-top (A5) and the backfill top (A3). In the sea-side it is considered at the bottom sand (A7), the CDM-bottom (A2) and the CDM-top (A1). The figures are produced from the final phases of acceleration-time histories that presented in Figs. 8 and 9. During the first shaking remarkable time lag is observed between the bottom and top of the ground in both the port-side (Fig. 10(a)) and sea-side (Fig. 11(a)). During the 45 Gal shaking time lag between the A7 and A5 is found in the port-side as 0.058 sec, whereas in the sea-side it is 0.067 sec (lag between A7 and A1). In the subsequent shakings (196, 294 and 343 Gal), time lags are varied in a narrow band both in the port-side and the sea-side. Average time lag of 0.135 sec in the port-side and 0.155 sec in the sea-side are observed. Acceleration in the bottom sand (A7), the clay top (A5) and the CDM top (A1) are considered in determining the time lags in both sides. In the first two shakings the shape of the waves remains almost sinusoidal but during the last two shakings spiky accelerations are observed in both sides. The initial stiffness of the system may be diminished by successive intense earthquake loading. However, limitation of the shaking table in large acceleration produces the spiky waves. This discussion implies that the phases of acceleration with time in the improved side are slightly different from the port-side, so that the horizontal pressures and the flexural stresses along the elevation of the sheet pile wall are different in both sides.

Earth pressure distribution

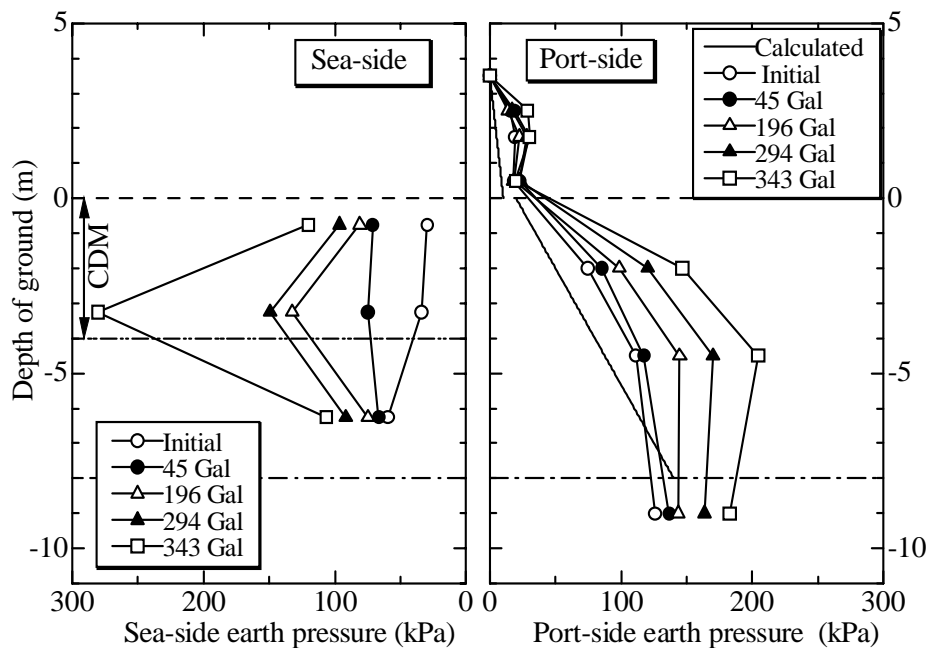


Figure12. Lateral earth pressure on the sheet pile quay wall

Horizontal earth pressures are measured with the earth pressure gauges installed on the sheet pile (Fig. 1). Figure 12 shows the earth pressure profile both in the sea-side and port-side at every shaking. Data is selected as the maximum value of last phase of each shaking. Calculated active earth pressure (Fig. 12, Okabe 1924) agrees well with the initial earth pressure. Earth pressure in the backfill (port-side) shows nonlinear variation. The active earth pressure increases consistently with the increases of acceleration. Trend of horizontal earth pressure in the sea-side is different from the port-side. Top two sensors (E11 and E10) in the sea-side were set inside the CDM block. It is seen from the figure that the middle sensor (E10) experiences larger pressure. The resisting force acting on the CDM may be much larger than that in the clay below the CDM. Shorter drainage path from the top (E11) and bottom earth pressure gauge (E9) can affect such pressure profile. However the earth pressure profile

in the sea-side is quite natural. It has been found from the data analysis that some residual pressure is accumulated after each shaking in the deeper part of the clay (E10 and E9). During the 343 Gal shaking the sea-side earth pressure obtained from E10 shows the effect of the residual pressure more.

Bending moments and structural deflection

Bending moments are derived from the responses of the strain gauges (S) along the sheet pile wall (Fig. 1). Figure 13(a) shows the bending moment of the sheet pile quay wall. Almost similar pattern of bending moment is developed in all of the shakings. Maximum bending moment is observed below the ground level and its magnitude is about 660 kN-m. The maximum bending moments in pseudo-static studies (Khan et al., 2006) took place at the ground level. Although the CDM zone in the sea-side is relatively stiffer than the port-side clay, the dynamic active earth pressure from the backfill and the clay is much larger than the resistance by the CDM. Due to firm fixation by the bottom dense sand and mobilized active pressures, the sheet pile wall starts to bend at bottom of the clay layer (Fig. 4(b)). Seaward rotational movement of the CDM block is also observed. Due to the extended part of sheet pile wall and cables on the top, smaller bending moments are developed at the backfill level.

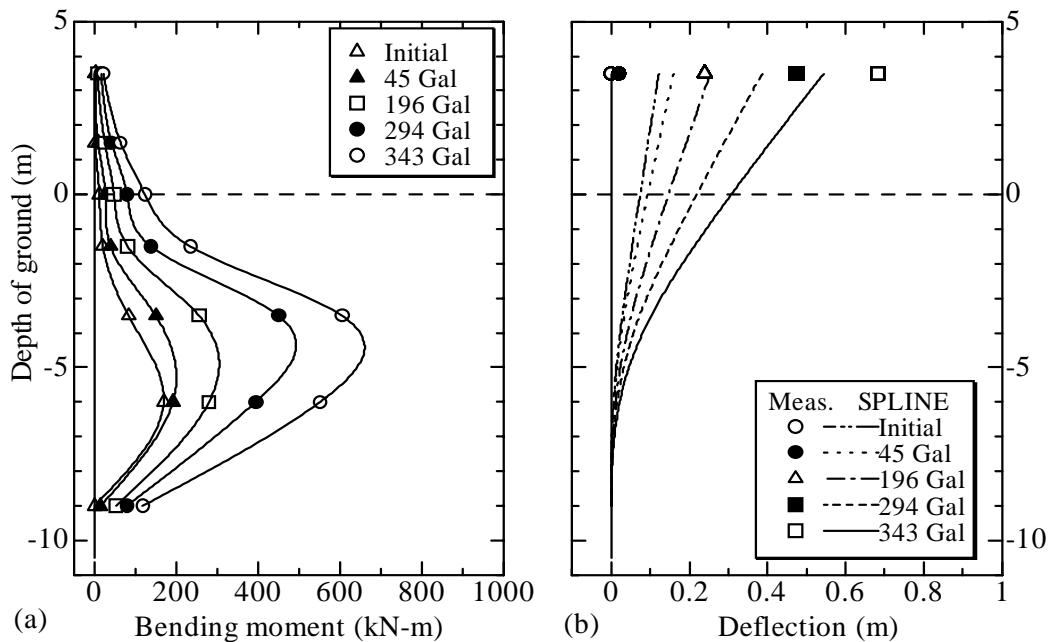


Figure 13. Bending moment and deflection distribution of quay wall

Quantic spline functions are used to fit the bending moment distribution. The marks in the bending moment curve (Fig. 13 (a)) are test data and the curve itself from spline equations. Two successive integrations of this curve lead to the determination of the lateral deflection along the wall, which is shown in Fig. 13(b). From the deflection distribution of the sheet pile quay wall firm fixity at the bottom part, the gradual bending at the clay bottom and the maximum displacement at the top can be visualized. Test data of deflection at each shaking agrees well with the plot of deflection distribution in Fig. 13(b).

CONCLUSIONS

A sheet pile quay wall with sea-side ground improvement has been investigated with reference to the load-deflection behavior, seismic responses, bending moment and earth pressure distribution in a centrifuge shaking table test. The conclusions of the study are as follows:

1. Centrifuge model of a sheet pile quay wall with sea-side ground improvement is successfully established.
2. Acceleration motion is found consistent from the base to the top of the sheet pile quay wall system and is different in each shaking.
3. Phases of acceleration in the improved side are slightly different from the port-side.
4. Excess pore pressure ratio is much smaller than unity, i.e., no liquefaction has taken place. Excess pore water pressure dissipates quickly, though some amount of the residual pore water pressure remains in the clay.
5. The maximum bending moment of the quay wall takes place approximately at the mid of the embedded depth. Little rotational movement of the CDM block was also observed.

REFERENCES

- Coastal Development Institute of Technology (CDIT), Japan. The deep mixing method - principle, design & construction, Rotterdam, Balkema. 2002.
- Khan, MRA, Hayano, K. and Kitazume, M., "Effects of sea-side ground improvement on the stability of existing sheet pile quay walls," Proc. 6th International Conference on Physical Modelling in Geotechnics, (Eds., Ng, Zhang and Wang), Vol. 2, pp. 1087-1093, Hong Kong, August 2006.
- Kitazume, M., Sato, T., Shiraishi, N. and Okubo, Y., "Failure pattern and earth pressure of locally cement improved ground under earthquake motion," Proc. International Conference on Physical Modelling in Geotechnics, (Eds., Phillips, Guo and Popescu), pp. 581-586, St. John's, Canada, July 2002.
- Mayne, PW and Kulhawy, FH, " K_0 – OCR relationships in soil," Journal of Geotechnical Engineering Div., ASCE, Vol. 108, No. G76, pp. 851-872, 1982.
- Okabe, S., "General theory on earth pressure and seismic stability of retaining wall and dam," Journal of Japan Society of Civil Engineers, Vol. 10 (6): 1277-1323, 1924.
- Stewart, DP, Chen, YR. and Kutter, BL, "Experience with the use of methylcellulose as a viscous pore fluid in centrifuge models," Geotechnical Testing Journal, GTJODJ: Vol. 21, No. 4, pp. 365-369, 1998.
- Watabe, Y., Imamura, S., Hirano, T., Kishi, M. and Yamamura, K., "Seismic performance of anchored sheet pile quay wall," Proc. 6th International Conference on Physical Modelling in Geotechnics, (Eds., Ng, Zhang and Wang), Vol. 2, pp. 1119-1124, Hong Kong, August 2006.
- Wroth, CP, "The interpretation of in situ soil tests," 24th Rankine lecture, Geotechnique, Vol. 34(4): 449-489, 1984.